

Review article

Evolution of tectono-sedimentary systems in the Kumano Basin, Nankai Trough forearc



G.F. Moore ^{a,*}, B.B. Boston ^a, M. Strasser ^b, M.B. Underwood ^c, R.A. Ratliff ^d

^a Department of Geology and Geophysics, University of Hawaii, Honolulu, HI 96822, USA

^b Geological Institute, ETH Zurich, 8092 Zurich, Switzerland

^c Department of Earth and Environmental Sciences, New Mexico Institute of Mining and Technology, Socorro, NM 87801, USA

^d Ratliff Geological Consulting, LLC, 75 Qualla Ct., Boulder, CO 80303, USA

ARTICLE INFO

Article history:

Received 12 December 2014

Received in revised form

18 May 2015

Accepted 19 May 2015

Available online 14 June 2015

Keywords:

Nankai Trough

Forearc basin

Tectonics and sedimentation

Integrated Ocean Drilling Program

ABSTRACT

Sedimentary deposits in the distal Kumano forearc basin of the Nankai accretionary margin off Kii Peninsula, Japan, have been imaged using three-dimensional (3D) seismic data. The seismic data, along with logging and core data from the Integrated Ocean Drilling Program (IODP) show that the unconformity between the accretionary prism and overlying forearc sediments is time-transgressive. The unconformity at Site C0002 separates 5 Ma prism rocks from 3.65 Ma basin deposits; at Site C0009 it separates 5.6 Ma prism from 3.8 Ma basin sediments. Acoustic reflections in the basal deposits are sub-parallel to the underlying accretionary prism; the acoustic facies varies in thickness from 50 to 750 m. The mudstone deposits and laterally equivalent turbidites are interpreted as lower trench-slope deposits. The condensed slope sediment (SS) section decreases in age from 3.5 to 1.5 Ma at Site C0002 to 1.5–0.9 Ma at C0009.

Acoustic sequences within the lower forearc basin (LFB) contain higher proportions of silt and sand turbidites and progressively onlap the SS unit along a low-angle discontinuity (KL) in a landward direction. Because of the landward onlap of the LFB unit, the oldest LFB strata at C0002 are older than 1.67 Ma, whereas those at C0009 are younger than ~0.9 Ma. Thus, the amount of time missing or characterized by condensed sedimentation across the KL unconformity decreases in duration in the landward direction. The landward-onlapping sequences tilt progressively landward in response to regional uplift along an out-of-sequence thrust (OOST; mega-splay) fault. Regional tilting shifted the basin's depocenter progressively landward, expanding that part of the basin from ~10 km in width to >30 km. The onset of sand-silt turbidite deposition in the distal basin began after more accommodation space was created by the uplift of the outer ridge along the splay fault at ~1.9 Ma. Conversely, turbidites of the Upper Forearc Basin (UFB) progressively onlap LFB in a seaward direction. Furthermore, the respective thicknesses of the LFB and UFB units switch from the seaward side of the basin (C0002) farther landward (C0009): the LFB unit is > 800 m thick in the seaward region, whereas it is only 200–300 m thick in the landward region; the UFB unit is < 50 m thick in the seaward region, and up to 600 m thick in the landward region. Thus, Kumano Basin responded in both space and time to a complex interplay between tectonics and sedimentation. The stratigraphy records a balance between the effects of prism uplift along the basin's distal edge with the rerouting of channels and canyons along the basin's proximal edge.

© 2015 Elsevier Ltd. All rights reserved.

1. Introduction

Forearc basins (FABs) are integral features along most convergent margins. Their sedimentary sections record the history of arc massif unroofing and evolution as well as the history of deformation of the seaward edge of the overriding plate. The stratigraphic sequences in such basins reflect the interactions between

* Corresponding author.

E-mail address: gmoore@hawaii.edu (G.F. Moore).

sedimentation, tectonics, climate, and sea level fluctuations. Although studies of exhumed FAB deposits, such as the Great Valley Sequence of California (e.g., Mitchell et al., 2010; Williams and Graham, 2013) provide insights into sediment accumulation and facies architecture, the controls on sedimentation in ancient FABs remain poorly documented because of the low-preservation potential and imprecise temporal resolution (Ingersoll and Busby, 1995). Many geophysical studies of modern FABs have utilized regional seismic reflection profiles to map the stratigraphic framework (e.g., Ballesteros et al., 1988; Beaudry and Moore, 1985; Berglar et al., 2008; Chapp et al., 2008; Coulbourn and Moberly, 1977; Laursen et al., 2002; Laursen and Normark, 2003; Matson and Moore, 1992; McNeill et al., 2000; Speed et al., 1989; Susilohadi et al., 2005; Torrini and Speed, 1989). Paquet et al. (2011) completed a high-resolution study of the Hawke Bay FAB (Hikurangi margin) that included precise integration of sequence-bounding unconformities and eustatic sea-level history. Most such basins, however, lack drilling data to provide sufficient age constraints and ground-truth for interpretation of seismic facies. With hydrocarbon exploration moving into deeper water, forearc basins are receiving more attention as viable petroleum systems (e.g., Struss et al., 2008; Lutz et al., 2011), and some are targets for commercial utilization of gas hydrates (Fuji et al., 2009; Tsuji et al., 2009). Thus, from both process-oriented and resource-driven perspectives, a holistic assessment of Kumano FAB in the Nankai Trough subduction system (Fig. 1) might yield insights regarding global commonalities and site-specific idiosyncrasies.

In this paper, we use 3D seismic reflection data calibrated with Integrated Ocean Drilling Program (IODP) core and log data to interpret the tectonostratigraphic evolution of the distal Kumano FAB. In addition to the two IODP sites drilled as part of the Nankai Trough Seismogenic Zone Experiment (NanTroSEIZE), the region

has been surveyed by numerous 2D seismic reflection and refraction lines, a 3D seismic survey, high-resolution multibeam bathymetry, and dozens of heat flow measurements. Integration of these data sets provides valuable insights into the stratigraphic architecture of sedimentary sequences and their connections to the regional tectonic and climatic evolution. This paper concentrates on the seaward portion of Kumano FAB, and complements comprehensive studies of stratigraphic controls on gas-hydrate distribution in the basin's NE corner (e.g., Tsuji et al., 2009; Noguchi et al., 2011; Takano et al., 2013; Egawa et al., 2013). Our goal is to tease apart the influences of accretionary-prism tectonics on shaping the basin's architecture as opposed to climatic-eustatic controls on sediment influx to the basin. Both have undoubtedly modulated the history of sedimentation, so we take a regional-scale view of the entire system with a more detailed focus on the young, distal portion of the basin.

2. Tectonic setting of the Nankai Trough

Along southern Japan, the Philippine Sea plate (PSP) subducts to the northwest beneath the Eurasian plate at a rate of $\sim 4.1\text{--}6.5\text{ cm yr}^{-1}$, forming the Nankai Trough (Fig. 1; Seno et al., 1993; Miyazaki and Heki, 2001). The current phase of convergence along this boundary probably began at $\sim 6\text{ Ma}$ (Kimura et al., 2014). Prior to the Miocene migration of a triple junction, convergence had been between the Pacific Plate and southern Japan, producing the Cretaceous-Miocene accretionary complex of the Shimanto Belt (Taira, 2001; Pickering et al., 2013; Raimbourg et al., 2014). Together, the various accretion phases along the margin have built a wide prism that extends more than 200 km from the central Shikoku/Kii Peninsula region to the trench (Fig. 1).

The Nankai system represents one end of the accretion-erosion continuum, characterized by accretion of thick accumulations of sediment ($>1000\text{ m}$). Broadly similar conditions exist in the Cascadia Basin, the Aleutian Trench, the Sunda Trench, and southern Chile (see Underwood and Moore, 2012 and references therein). Sediment is now actively accreting at the deformation front, with all of the trench sediments and at least half of the underlying sedimentary section of the Shikoku Basin (northern PSP) typically being accreted at the toe of the prism along its strike length (e.g., Aoki et al., 1982; Moore et al., 1990). Several prominent forearc basins have developed along the strike of the margin (Tosa, Muroto, Kumano; Fig. 1). Within the Kii-Kumano corridor, a large volume of the lower Shikoku Basin strata has been underthrust beneath the seaward edge of the Kumano FAB (Bangs et al., 2009). That decoupling of the subduction inputs is related to out-of-sequence thrusting along a regional megasplay fault that has uplifted a broad ridge, behind which the FAB has formed (Park et al., 2002).

The Shikoku Basin is the main sedimentary system on the northern part of the subducting Philippine Sea plate. The basin formed during the late Oligocene to late Miocene by rifting and back-arc spreading behind the Izu-Bonin arc system (Okino et al., 1994; Kobayashi et al., 1995; Sdrolias et al., 2004). Shikoku Basin is characterized by both regional and local variations in basement relief, sediment thickness, and sedimentary facies (Ike et al., 2008a, 2008b). Seamounts on the subducting plate have been imaged under the Nankai forearc region (Park et al., 1999; Kodaira et al., 2000). Subduction of the basement highs can cause significant deformation in the upper plate (e.g., von Huene, 2008; Kimura et al., 2011) and shift the stratigraphic position of the plate interface.

The outer or frontal accretionary prism of the Nankai system is actively deforming (Screaton et al., 2009), with deformation concentrated near the toe of the prism (Fig. 2). The boundary between the outer prism and the inner prism (Wang and Hu, 2006)

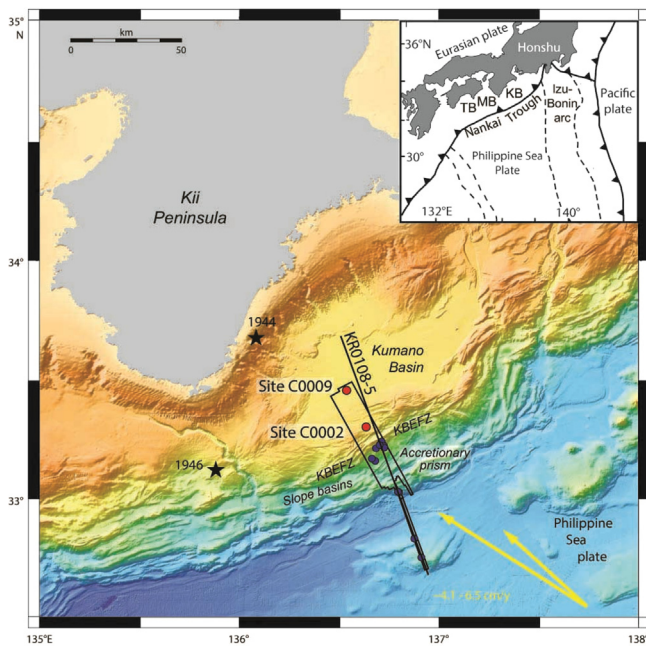


Fig. 1. Regional location map. Red dots = IODP drill sites used in this paper, blue dots = other NanTroSEIZE drill sites. Black outline = region with 3-D seismic data; yellow arrows = estimated far-field vectors for motion of Philippine Sea Plate (PSP) with respect to Japan (Seno et al., 1993; Heki, 2007). Stars = epicenter locations of 1944 and 1946 tsunamigenic earthquakes. Black line = KR0108-5 seismic reflection line shown in Fig. 2. KBEFZ = Kumano Basin Edge Fault Zone (Martin et al., 2010). Inset in upper right is regional location map – KB = Kumano Basin; MB = Muroto Basin; TB = Tosa Basin.

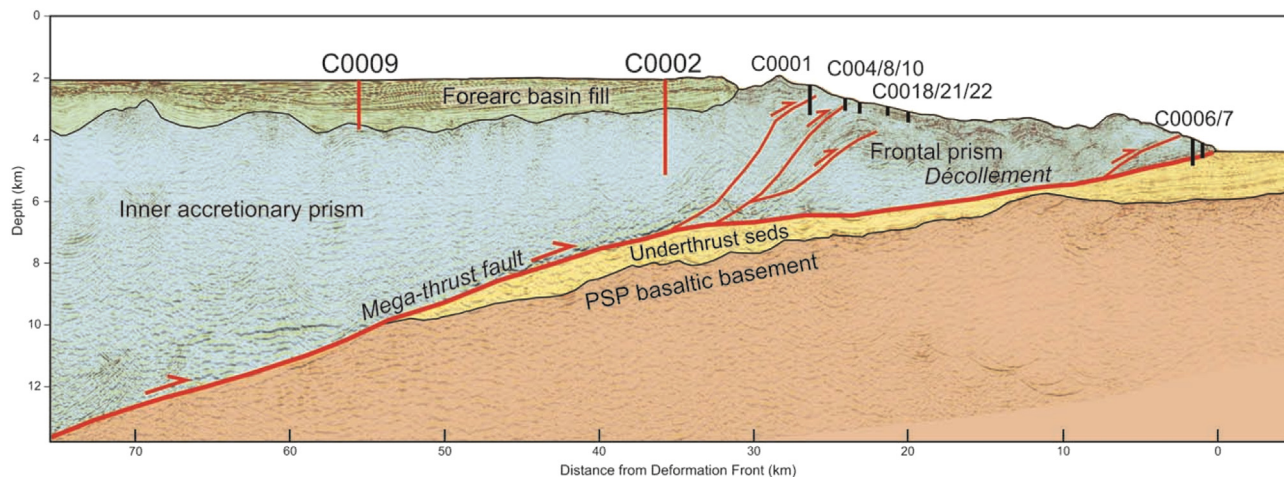


Fig. 2. Regional 2-D seismic line KR0108-5, showing IODP Sites used in this paper (red) in relation to all other NanTroSEIZE drill sites (black). PSP = Philippine Sea Plate. Location shown in Fig. 1. Modified from Park et al. (2002), Nakanishi et al. (2008), and Moore et al. (2014).

within the NanTroSEIZE transect area is the Kumano Basin edge fault zone (KBEFZ), and the Kumano forearc basin lies atop the inner prism (Fig. 3; Moore et al., 2009; Martin et al., 2010). The Kumano Basin is a classic “ridged”, accretionary FAB (e.g., Dickinson, 1995) that is deposited on a Miocene-Pliocene accretionary complex (Underwood and Moore, 2012). It is bounded on its landward margin by an older accretionary prism and anomalous near-trench plutons (Shimanto Belt; Taira et al., 1988; Kimura et al., 2014) and on its seaward margin by the crest of the active accretionary prism and the KBEFZ, a zone of complex normal and strike-slip faulting (Martin et al., 2010). The basement of Kumano Basin is composed of deformed upper Miocene and older accretionary

prism rocks that are unconformably overlain by lower Pliocene trench slope deposits (Kinoshita et al., 2009). The uplift along a regional OOST that began around 1.95 Ma (Strasser et al., 2009) is thought to have created the accommodation space for accumulation of thick forearc-basin deposits near the basin’s distal edge in the Kumano transect (Underwood and Moore, 2012).

Quaternary sediment has been routed into Kumano Basin from the Kii Peninsula and regions to the east on Honshu via both large and small submarine canyons (Fig. 3) and slope failures that funnel turbidity currents to the basin floor (Kawamura et al., 2009; Shirai et al., 2010; Omura et al., 2012; Egawa et al., 2013; Shirai and Hayashizaki, 2013). The distal forearc basin strata in the Kumano transect are all Quaternary (<2 Ma) in age (Kinoshita et al., 2009; Saffer et al., 2010).

More than 3 km of basin-filling sediment has been tilted landward, presumably due to continued slip on the megasplay fault (Park et al., 2002; Gulick et al., 2010; Hayman et al., 2012). This activity postdates an earlier phase of asymmetric forearc high uplift (strongest uplift in the southwestern part of the Kumano transect; Fig. 4) that may have occurred in concert with splay fault steepening and underthrusting of a large volume of sediment beneath the thrust [Bangs et al., 2009].

Near the basin’s distal edge, strata are cut by numerous normal faults, many of which offset the seafloor (Fig. 2; Park et al., 2002; Gulick et al., 2010). At least three generations of normal faults cut the FAB strata, but vertical offsets are generally less than 20 m and the overall horizontal extension in the seaward part of the basin is less than 2% (Moore et al., 2013; Sacks et al., 2013). Thus, late-stage extensional faulting probably had little influence on patterns of sedimentation.

3. Data and methods

3.1. 3D seismic data

Our primary regional data set is a 3D seismic reflection volume that was collected by Petroleum GeoServices (PGS) across the Kumano Basin and Nankai accretionary prism SE of Kii Peninsula in 2006 (Fig. 1; Moore et al., 2007, 2009). The 12-km wide, 56-km long survey area covered the region from the trench axis landward into the Kumano Basin. The data set was acquired with a commercial seismic vessel towing two airgun source arrays (each totaling 3090 cu in) and four 4.5 km long hydrophone streamers. Basic processing

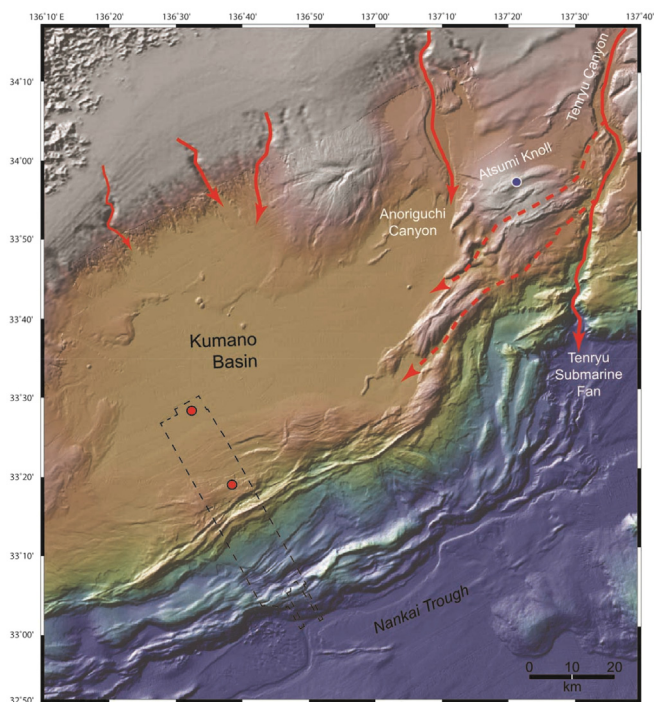


Fig. 3. Kumano Basin area with major sediment dispersal pathways shown in red (present = solid line, possible past pathways = dashed lines; Egawa et al., 2013; Noguchi et al., 2011; Takano et al., 2013; Usman et al., 2014). Red dots are IODP drill sites, blue dot is Atsumi Knoll drill site.

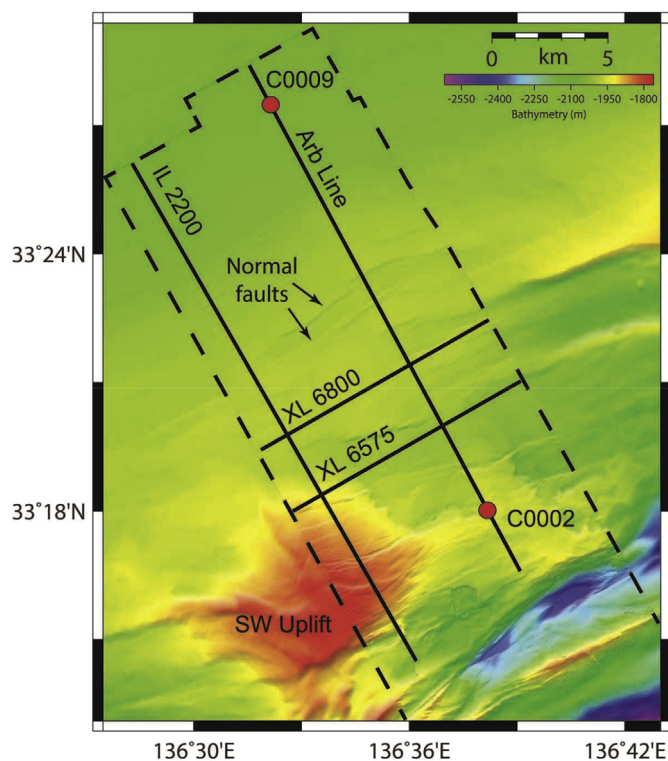


Fig. 4. Details of high-resolution bathymetry of our study area with color table optimized to show the Southwest Uplift. Dashed line shows location of 3D seismic survey; solid lines show locations of seismic inlines and crosslines shown in later figures.

through pre-stack time migration was performed by Compagnie Générale de Géophysique (CGG) and full 3D pre-stack depth migration (3D PSDM) was completed by the Japan Agency for Marine Earth Science and Technology (JAMSTEC). See details of processing procedures in Moore et al. (2009). The interval between inlines (oriented NW–SE) and cross lines (oriented SW–NE) of the resulting dataset is 18.75 m and 12.5 m, respectively. The vertical resolution for the interval of interest in this study is between 5 and 20 m (i.e. 5–7 m near the seafloor, 10–20 m at depths near 1400 mbsf (Moore et al., 2009).

Gulick et al. (2010) divided the distal basin's seismic stratigraphy into two main units, a lower unit that unconformably overlies an inferred older accretionary prism and an upper unit that progressively onlaps the lower unit in a landward direction. The upper unit comprises twelve seismic stratigraphic sequences that are gently tilted landward, and is the major focus of this paper. The upper boundaries of these sequences are key seismic horizons that we mapped throughout the study area using standard seismic-stratigraphic mapping tools implemented in the *Paradigm* seismic interpretation software package. Young normal faults and a bottom-simulating reflection (BSR) caused by gas hydrate accumulations (Miyakawa et al., 2014) obscure some relationships and hamper interpretations. Several horizons were interpolated through the BSR because the seismic amplitudes of the horizons were complicated by free gas associated with the base of gas hydrate zone.

Isopach maps were constructed by first gridding and smoothing our 12 picked seismic horizons. Isopachs are true stratigraphic thickness calculated by finding a normal at each grid cell at the top horizons and measuring the distance to the bottom horizon. Because deeper horizons (K5–K12) onlap onto horizon KL and do not extend to the NW terminus of the survey, we merged each deep horizon with horizon KL to produce the bottom boundary of the

isopachs. Thus, the top boundary defined the NW extent of those isopachs.

We used the structural restoration software LithoTect[®] to model and restore the frontal wedge interpretation to a viable restored state geometry. Flexural slip kinematics were applied for both restoration and iterative forward modeling, preserving bed lengths and unit areas (Geiser et al., 1988; Groshong et al., 2012; Rowan and Ratliff, 2012). Fault prediction, also using the flexural slip kinematic model (Geiser et al., 1988), was used to calculate the trajectory of the OOST (splay) fault that produced the landward tilted forearc basin horizons. The predicted fault trajectory is consistent with the internal wedge seismic reflector characteristics, and soles into the same primary detachment level as appears to be responsible for the frontal imbricate structures.

3.2. IODP core data

In order to investigate the temporal and spatial evolution of Kumano Basin, and to study how its behavior near the distal edge relates to the overall tectono-stratigraphic evolution and splay fault activity, we integrate the 3D seismic data with age constraints from cores, cuttings and logs taken at IODP Sites C0002 and C0009 (Expedition 315 Scientists, 2009; Expedition 316 Scientists, 2009; Expedition 319 Scientists, 2010; Strasser et al., 2014) (Figs. 5 and 6). Underwood and Moore (2012) summarized age data from cores in the upper and lower parts of the stratigraphic section (Expedition 315). Additional data to fill a coring gap from the middle of the basin's stratigraphic section were collected during Expedition 338 (Strasser et al., 2014).

4. Tectono-stratigraphic units of Kumano forearc basin

We have identified four tectono-stratigraphic units in the seismic data that have been characterized by coring and logging. The deepest unit is strongly deformed with little seismically-defined structure. Core data indicate this unit is an accretionary prism (AP; Expedition 315 Scientists, 2009). Overlying the deformed prism is a folded unit of mudstone interpreted as lower trench-slope sediments (SS). The slope sediments are in turn overlain by two landward-tilted units of the Quaternary forearc basin (Lower Forearc Basin – LFB and Upper Forearc Basin – UFB).

Coring into the accretionary prism during Expedition 315 was hampered by poor recovery but showed that the accretionary prism sediments consist mostly of indurated, highly fractured mudstone, siltstone, and sandstone, with rare carbonate-cemented nodules. Low contents of calcium carbonate in the mudstone indicate deposition close to or below CCD (Expedition 319 Scientists, 2010). The top of the accretionary prism becomes older in the landward direction: at Site C0002 the prism strata are 5.0 Ma to 5.6 Ma, but are 5.59 Ma to >7.88 Ma at Site C0009. Subsequent riser drilling showed that the deeper strata at Site C0002 are older: the interval from ~2145.5 to 2945.5 mbsf has a depositional age of 9.56–10.73 Ma based on nannofossil first and last occurrence data (Expedition 348 Scientists, 2014). The original depositional environment (i.e., prior to accretion) is difficult to pinpoint but probably consisted of a relatively fine-grained part of the paleo-trench wedge (Expedition 315 Scientists, 2009). The upper surface of the accretionary prism displays an uneven geometry on the seismic profiles (Figs. 7A, 8 and 9). The boundary has small-scale (few 10's of meters) roughness and undulates at scales of 0.5–5 km. The undulations are thought to be the tops of thrust packets with fault-bend folds within the prism, modified by slumping as exemplified by the modern lower slope environment (Strasser et al., 2011).

Above the prism sits a highly variable unit that ranges in acoustic character from relatively transparent and measuring

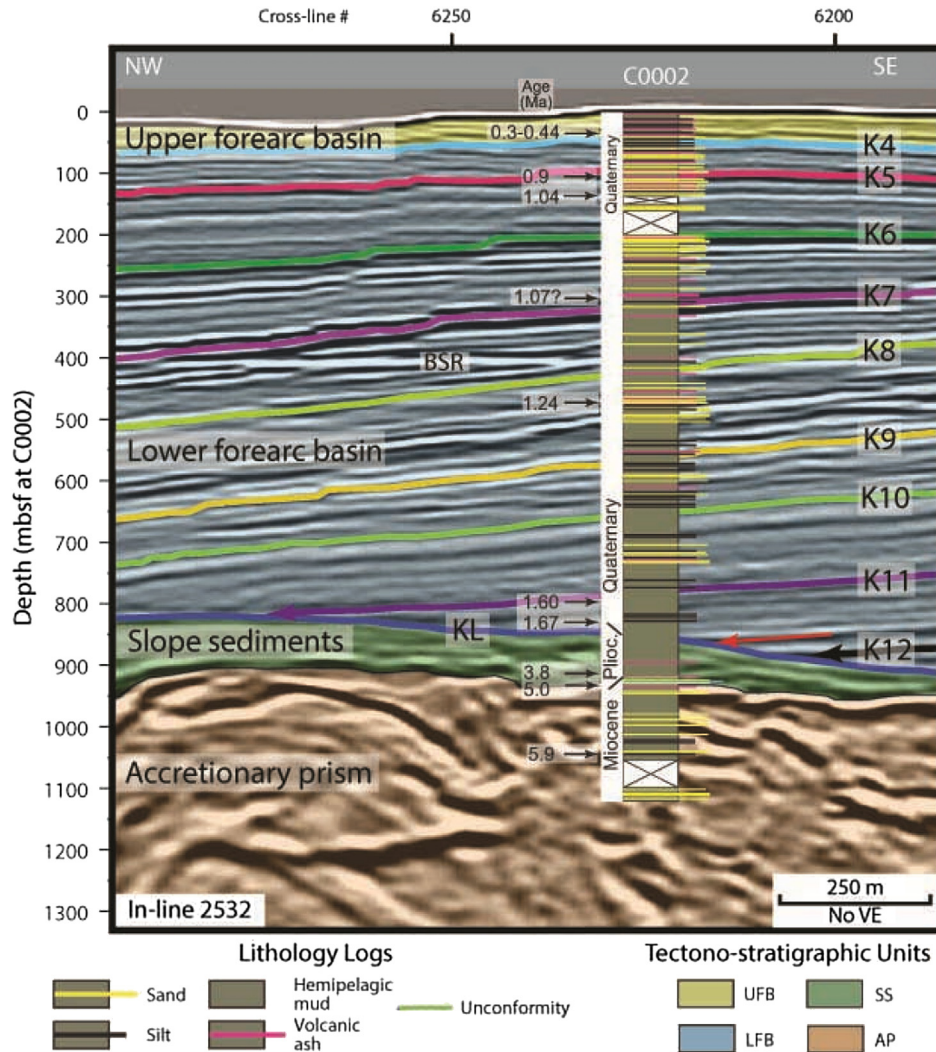


Fig. 5. Lithostratigraphic summary column of Site C0002 overlain on a 3D seismic in-line. Seismic sequence boundaries are from Gulick et al. (2010). Labeled seismic horizons are the tops of sequence boundaries as defined by Gulick et al. (2010); e.g., KL = top of “Kumano Lower”, K11 = top of “Kumano 11”. VE = vertical exaggeration.

~50–100 m in thickness at Site C0002 (Fig. 5), to strongly stratified with thicknesses as great as 750 m near Site C0009 (Fig. 6). Locally, the transparent interval dips seaward, and in other places it fills topographic lows in the underlying prism. This geometry and acoustic character are consistent with hemipelagic and turbidite sedimentation in basins on the lower trench slope (Moore et al., 2009; Expedition 315 Scientists, 2009). Equivalent deposits have been cored in slope basins elsewhere in the Nankai forearc (e.g., Underwood et al., 2003). Coring at C0002 confirmed that a condensed section of clay-rich hemipelagic deposits is separated from the underlying prism by an angular unconformity, with a corresponding hiatus spanning ~1.2 Ma. Strata above the unconformity are 3.79 Ma to 1.67 Ma, and rates of sedimentation within that condensed section were only 18–30 m/Ma. The content of calcite averages ~16 wt-% in the mudstone, which indicates deposition above CCD. Along strike to the NE (Atsumi Knoll; Fig. 3), cores from gas-hydrate exploration wells document significant accumulation of sandy turbidites in braided channels and fans with ages as old as 2.4 Ma within the slope sediment section (Noguchi et al., 2011; Takano et al., 2013). Further details of the origin and evolution of the slope sediment unit are addressed by Ramirez et al. (2015), who subdivided SS into three subunits.

The slope sediment (SS) tectono-stratigraphic unit can be traced landward to Site C0009, where the slope sediments are more than five times thicker than at C0002. Deposition at Site C0009 occurred between ~3.8 and ~1.34 Ma (Expedition 319 Scientists, 2010). Here, the facies is more diverse. The lower part (Unit IIIB) contains abundant wood/lignite fragments that correlate with high TOC and methane concentrations. There are traces of ethane and propane, but the molecular composition of hydrocarbons suggests a microbial source of natural gas (Expedition 319 Scientists, 2010). Farther landward in the Kumano Basin, molecular ratios and carbon isotopic compositions indicate hydrocarbon derivation from thermal cracking of organic matter (Pape et al., 2014). The upper part of the facies at C0009 (Unit IIIA) is younger than ~2.5 Ma (Kameo and Jiang, 2013), and sedimentation rates are comparable to the condensed section at C0002.

The seismic stratigraphic sequences defined by Gulick et al. (2010) through most of the distal basin fill are sufficient to map the development of the basin, so we adopt their terminology (Figs. 5 and 6). Labels K1 through K12 are the horizons that define the tops of the seismic sequences. We here group by geometric similarity seismic sequences K1 through K3 as “Upper Forearc Basin” (UFB) and sequences K4 through K12 as “Lower Forearc Basin”

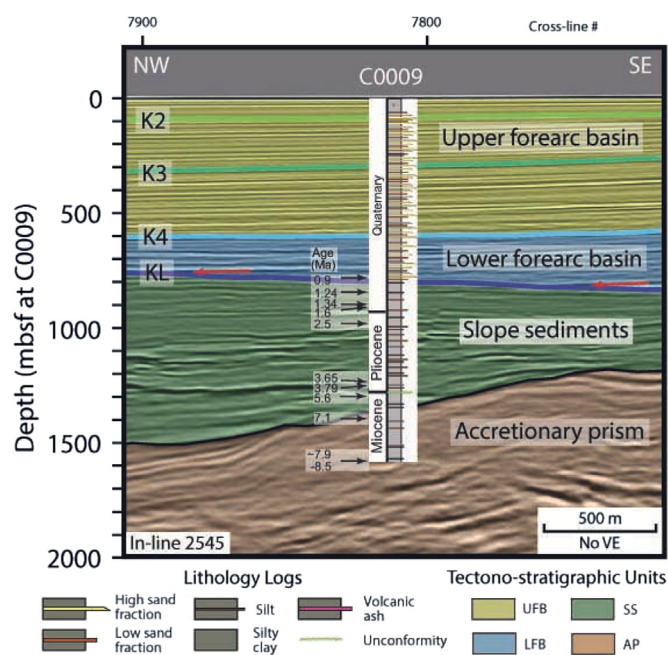


Fig. 6. Lithostratigraphic summary column of site C0009 overlain on a 3-D seismic in-line. Seismic sequence boundaries are from Gulick et al. (2010). VE = vertical exaggeration.

(LFB), which differs from the lithologic designations given by Expedition 315 scientists (2009) and Expedition 319 Scientists (2010). Sequences of the LFB progressively onlap the Slope Sediments (SS) toward land along an onlap unconformity. That boundary was designated Kumano Lower (KL) by Gulick et al. (2010) and surface S2 by Expedition 319 Scientists (2010).

The onset of silty turbidite sedimentation in the Quaternary forearc basin is constrained by the age just above the KL horizon (Figs. 5 and 9); that age is about 1.67 Ma at Site C0002. The oldest seismic sequence in the Quaternary forearc basin is K12, which is restricted to a narrow trough at the seaward edge of the basin (Fig. 9). Uplift of the seaward boundary is apparent from the tilt of the deepest sediments and their onlap relationships along horizon KL.

This sequence boundary is time transgressive with younger strata onlapping toward land. Thus, the lower part of Sequence 11 and all of Sequence 12 at the seaward edge are older than strata that onlap at Site C0002. The thickness of this K11-KL interval is ~300–325 m (Fig. 9). If we assume a constant sedimentation rate consistent with that of Unit II at C0002 (~1000 m/Ma), this lower interval represents 0.30–0.32 My of time. Thus, the onset of rapid basin sedimentation seaward of C0002 would be ~1.95–2.0 Ma. That timing broadly coincides with the initiation of the megasplay fault as an out-of-sequence thrust (Strasser et al., 2009).

The uppermost part of the SS unit is a condensed section all along the onlap unconformity (Fig. 7C). Because of the landward onlap of the LFB unit, the oldest basin strata in the most seaward region of the basin are older than 1.67 Ma, whereas facies equivalents near Site C0009 are younger than ~0.9 Ma (Fig. 7C). Thus, the amount of time missing or characterized by condensed sedimentation across the KL unconformity decreases in duration in the landward direction.

Sequences K12 through K8 are tilted landward ~6–7° and are generally uniform in thickness (Fig. 7). Sequences K7 through K5 also have maximum dips of ~6–7°; however, their dips decrease seaward. The change in dip is abrupt in the eastern side of the basin

(Fig. 7), but is more gradual in the west (Fig. 8). Sequences K8 through K12 mostly tilt the same amount, and K7 thins seaward, so tilting began at a time corresponding to the top of K8. Sequences K4–K6 all thin seaward.

The LFB seismic sequences are also tilted to the northeast along the SW uplift near the basin's seaward edge. This tilt is best seen in 3D seismic cross lines (e.g., Figs. 10 and 11). All units below K5 have approximately the same dips, while sequence K4 has some internal thinning due to onlap. Sequence 4 is in turn onlapped by sequence K3.

A group of normal faults mapped by Moore et al. (2013) are spatially correlated with the SW uplift and cut sequences K5 and K4, but the faults do not penetrate through the K4 sequence boundary (Fig. 11). That relation indicates that the uplift was relatively rapid and became inactive before the end of deposition of K4 (~0.436 Ma at Site C0009).

The relative thickness of the LFB versus UFB intervals switches from the seaward side of the basin (C0002) toward land (C0009). The LFB is > 800 m thick in the seaward region, but only 200–300 m thick farther landward (Figs. 5–7). The UFB is < 50 m thick in the seaward region, but up to 600 m thick farther landward. The grouped sequences of UFB and LFB are separated by an onlap unconformity that corresponds to the S1 designation of Expedition 319 Scientists (2010) and is equivalent to our sequence boundary K4. The discontinuity is best displayed in the western part of the basin (Fig. 8), where the SW uplift has caused a more abrupt angular discordance. Sequences K3 through K1 of UFB thicken landward and progressively onlap LFB in a seaward direction (Figs. 7 and 8). The region of tilting of sequences K3 through K1 has been shifted landward relative to the LFB sequences.

4.1. Regional development of tectono-stratigraphic units

Although we portray the distal portion of Kumano Basin in a series of two-dimensional (2D) cross-sections, the basin is not a simple 2D feature. There are significant along-strike variations in sedimentation and deformation. We created isopach maps for each seismic sequence (Fig. 12) to document the spatial and temporal variability. Strata of K9 through K11 are <200 m thick, < 5 km wide and are restricted to the SW part of the study area. The basin increases to 8–11 km in width and expands landward during deposition of K7 and K8 and further expands to 15–16 km in width during deposition of K5 and K6, with further landward expansion that reflects the onlap of these sequences onto the KL surface. The landward onlap is also reflected by the general landward thinning of sequences. The most dramatic change in sedimentation occurred during deposition of sequence K4 when the basin expanded beyond the NW edge of our survey. Deposition at that time was concentrated in a narrow (4 km wide) depression overlying the thickest accumulation of slope sediments of the underlying unit. The age interval spanned by sequence K4 at C0002 is ~0.9–0.44 Ma (based on the integrated age-depth model) and the maximum thickness is 570 m, yielding a sedimentation rate of 635–1295 m/Ma.

Maximum subsidence above the SS unit occurred during deposition of seismic sequence K4, with more than 600 m of sediment accumulation. Sequence boundary K5 is folded into a gentle syncline with landward dip at its seaward side and seaward dip on its landward side (Fig. 7). The onlap point, which must have been nearly horizontal during deposition, now dips seaward. Young horizons within sequence K4 are bowed up over the buried anticline. Landward of the fold, horizons within K4 again dip landward. Subsidence continued during K3, but to a lesser extent.

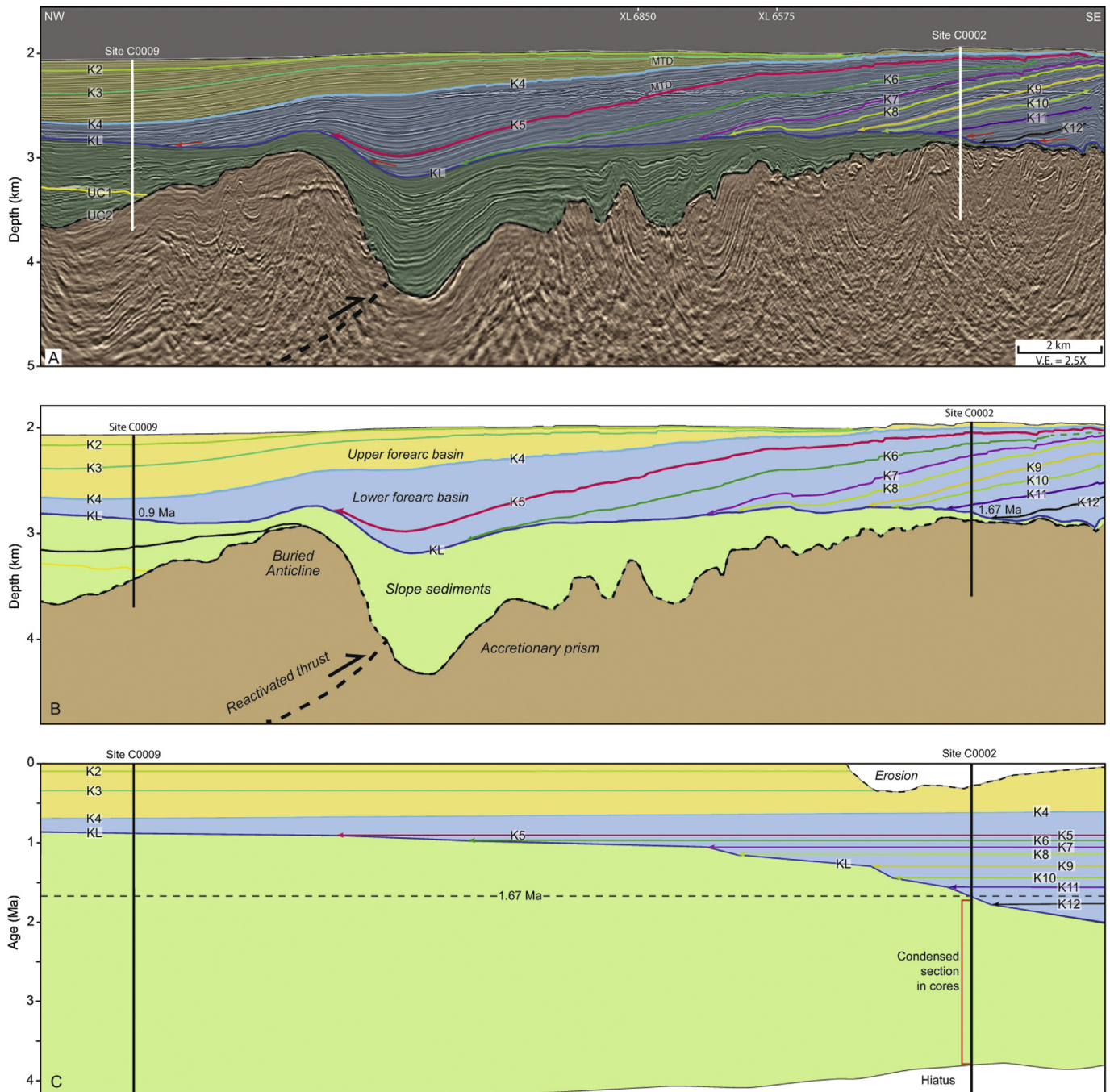


Fig. 7. Arbitrary seismic line through drill sites C0002 and C0009. Location shown in Fig. 4. Colors of tectono-stratigraphic units are the same as in Fig. 5 and 6. A. Interpreted seismic data. B. Correlation of seismic-stratigraphic sequence boundaries across the area. C. Chronostratigraphic diagram.

5. Discussion

5.1. Basin evolution

The architecture of the seaward half of Kumano Basin was controlled primarily by uplift along strands of the OOST (splay) fault system and secondarily by continued deformation of the underlying accretionary prism. Prior to ~2 Ma, the distal part of the system was a seaward-sloping outer accretionary wedge with slope sediments blanketing the slope and accumulating in structural lows (Fig. 13E). In contrast, to the NE of our transect (e.g., Atsumi Knoll), parts of the slope were sites of braided channel and

submarine fan deposition (Noguchi et al., 2011; Egawa et al., 2013) with lateral sediment feed, probably very similar to the Neogene Hikurangi forearc (Burgreen and Graham, 2014).

At ~2 Ma, an OOST broke through the outer prism, uplifting the outer ridge, generating more accommodation space for the nascent FAB and reconfiguring the distribution of depocenters. As silt and sand turbidites began to fill the seaward part of the basin (near Site C0002), they overlapped the condensed section of the SS units. Because sedimentation continued on the forearc slope of the study area (near Site C0009), although at a low rate of deposition, the condensed mudstone section continued to accumulate landward of the onlapping strata.

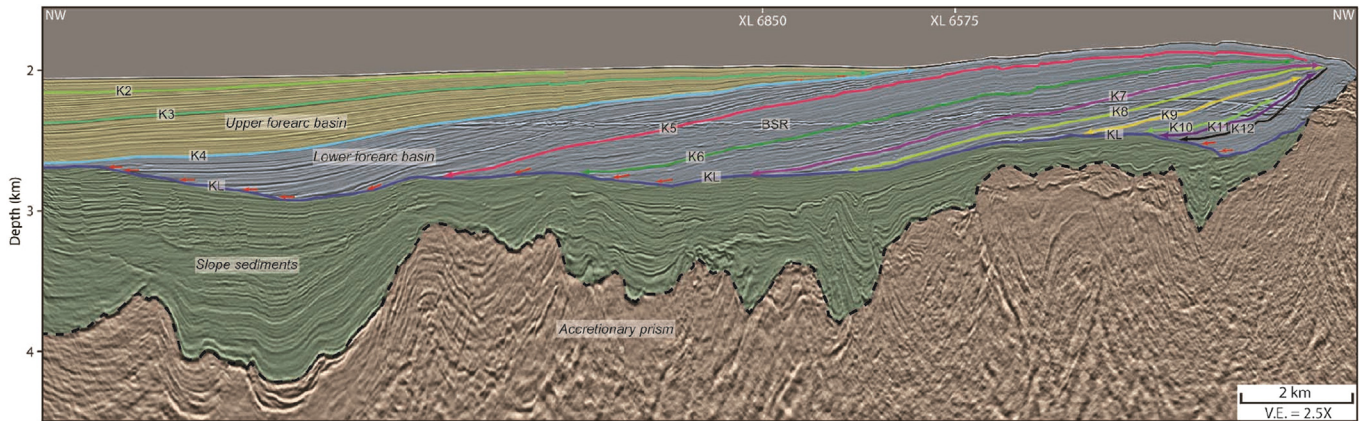


Fig. 8. Seismic InLine 2200 showing uplifted SW region. Location shown in Fig. 4. Colors of tectono-stratigraphic units are the same as in Fig. 5 and 6.

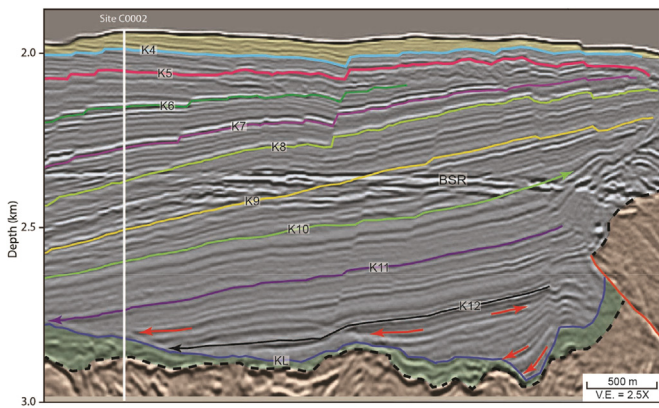


Fig. 9. Detail of the frontal part of the forearc basin section showing older sequences progressively onlapping the KL unconformity. Location shown in Fig. 4.

Motion along a new, more landward splay fault branch caused additional uplift of what would become the outer ridge of Kumano Basin, which in turn caused tilting of the sequences of the LFB (Fig. 13B). Tilting progressed over a relatively short time period, as tilting started ~1.2 Ma (top of sequence K8) and was complete by about 0.9 Ma (top of sequence K5), so 6–7° of tilt occurred in ~300 kyr. Our Lithotect modeling determined that ~4525 m of slip (1650 m of horizontal shortening) along the main splay fault branch

is required to produce that amount of landward tilt. During this same time interval, uplift also occurred along the southwest boundary of our 3D survey area (SW uplift in Fig. 4). Continued splay fault slip of ~1175 m caused landward tilt of sequences K4 and 3 (Fig. 13A). The isopach maps (Fig. 12) show widening of the basin as well as landward shifting of the basin depocenter in response to this tilting.

The tectonic development of the basin was affected by reactivation of a large buried anticline in the underlying accretionary prism section (Figs. 7 and 13B). Boston et al. (2011) interpreted this anticline as the hanging wall of a paleo-thrust that is similar to active thrusts on the active accretionary prism seaward of the Kumano Basin. An inferred paleo-slope basin with ~1000 m fill shows onlap of deep sediments against the major paleo-thrust indicative of a topographic high before sedimentation occurred (Fig. 7). Sequence K5 is folded by the thrusting beneath it, and sequence K4 is significantly thicker over the deeper basin, indicating that reactivation occurred between ~0.9 and 0.5 Ma. Mechanisms for the continued motion on, or reactivation of, this paleo-thrust are unclear but could involve fault interactions during the formation of the modern forearc basin, possibly caused by subduction of a seamount on the down-going Philippine Sea Plate, as has been suggested by Kimura et al. (2011) and Moore et al. (2013). Seamounts have been imaged under the Nankai prism (e.g., Park, 1999; Kodaira et al., 2000), and deformation due to seamount subduction has been suggested for other accretionary prisms (e.g., Kopp, 2011).

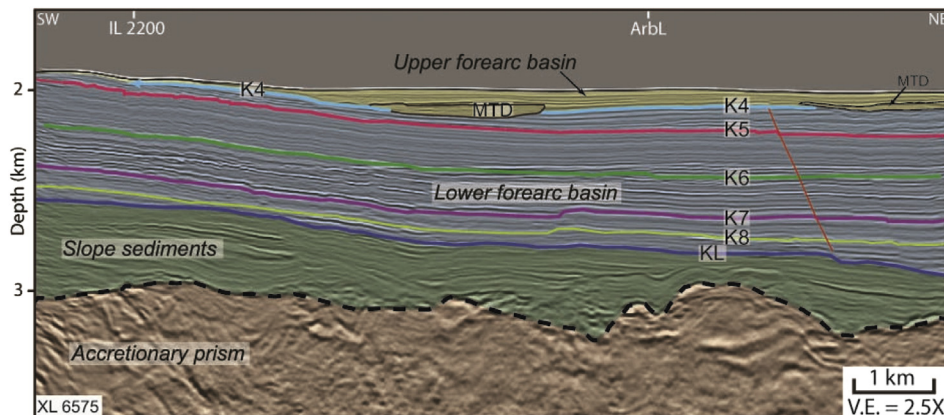


Fig. 10. Seismic XL 6575 showing NE tilt of sequences K4 through K8 with very thin sequences K3 and K4 overlying the tilted strata. Location shown in Fig. 4.

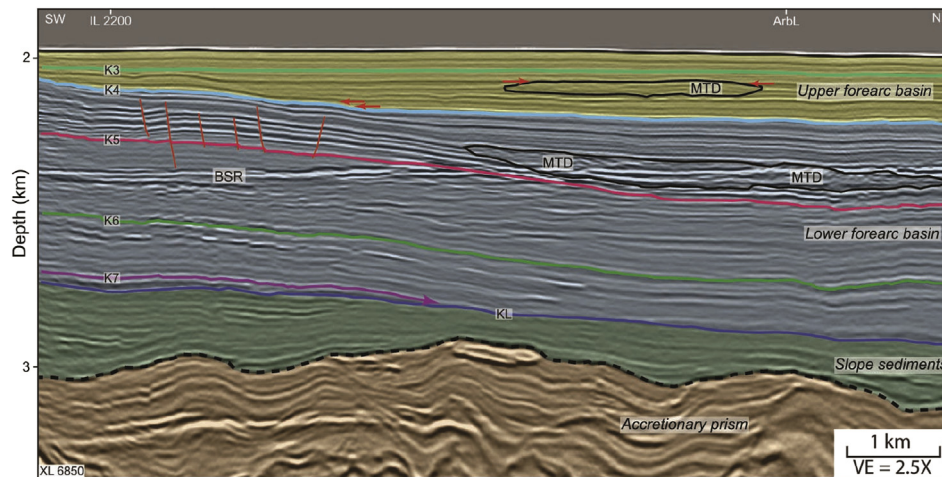


Fig. 11. Seismic cross-line (XL) 6850 showing NE-tilt of sequences K4 through K7 and thinning of sequences K2 and K3 over the uplifted region. Sequences K5 through K7 are all tilted the same amount, indicating that tilting occurred during deposition of sequence K4. Note mass-transport deposits MTDs within sequences K3 and K4, further described by Moore and Strasser (2015). Location shown in Fig. 4.

5.2. Basin sedimentation processes

The Kumano forearc basin has accumulated more than a kilometer of mixed terrigenous/hemipelagic sediments near its distal edge over the past 2.0 Myr. In addition to the distal turbidites, acoustic character indicates that extensive (>50 m thick, $\sim 5 \times 10$ km) mass transport deposits (MTDs) are common in the upper portion of the LFB section and in the lower portion of the UFB section (Figs. 10 and 11). These MTDs indicate transport direction from SE to NW (Moore and Strasser, 2015), and they were deposited during the time of tilting of the basin strata. Therefore, we attribute their origin to steeper landward-facing surface slopes that would have existed during the uplift stage, as well as dynamic loading by earthquakes that accompanied slip events. Many thinner and less extensive MTDs are present in deeper parts of the basins as well (Moore and Strasser, 2015).

The acoustic character of the distal turbidites consists of landward-tilted, high-amplitude, laterally continuous reflections. The turbidites lap onto the older, condensed-mudstone facies. Continuation of the uplift along the megasplay migrated the locus of sedimentation landward. Accumulation of significant volumes of sand in the distal basin–plain type environment depended on the creation of suitable accommodation space by accelerated uplift along the megasplay fault, but the frequency of transport by sandy and silty turbidity currents from the shoreline also depended on high rates of erosion in the hinterland and incision of an effective delivery system into the upper continental slope, as represented by the Quaternary network of through-going submarine canyons and slope gullies (Fig. 3).

The cyclic character of the distal turbidites (e.g., meso-scale cycles of sand frequency and sand thickness) was recorded in impressive detail by LWD data (Expedition 314 Scientists, 2009). Although age control from coring is not precise enough to verify Milankovich forcing (e.g., 100 kyr eccentricity cycles), we suspect that the meso-scale cycles were caused by eustatic sea-level fluctuations, with higher influxes of sand during lowstands. As indirect support for such contentions, Omura and Ikehara (2010) showed that depositional activity in the north part of Kumano Basin fluctuated during eustatic sea level changes. In addition, onland exposures of coeval forearc-basin deposits (Kazusa Group) record clear evidence of glacio-eustatic cyclicity (Pickering et al., 1999; Kazaoka et al., 2015).

Kumano Basin is not unique in these respects. The Hawke Bay forearc basin offshore New Zealand displays a similar retrogradational trend and arcward migration of depocenters (Paquet et al., 2011). Stratigraphic correlations and dating of those depositional sequences demonstrate a convincing relation to 100-kyr eccentricity cycles and associated eustatic fluctuations of sea level. The Hawke Bay system also evolved from a series of smaller ridge-parallel basins to a succession of larger amalgamated basins that progressively developed around major thrust-faulted ridges. Unlike distal Kumano Basin, the forearc deposits in Hawke Bay have been folded into several anticlines, which could provide structural closers for hydrocarbon accumulations. If hydrocarbons migrate up-dip across distal Kumano Basin, they probably discharge along a bathymetric notch near the seaward edge of the basin (Guo et al., 2013). Bangs et al. (2010) suggested that the “notch” was excavated ~ 0.05 Ma.

Present-day bathymetry around Kumano Basin provides a series of well-defined transverse delivery routes across the narrow shelf and upper slope (Fig. 3), but patterns of sediment dispersal seem to have shifted over time. To constrain the detrital provenance, several tracers (e.g., bulk modal percentages, heavy minerals, pyroxenes) have been used to compare sands from Sites C0002 and C0009 with those from modern river mouths on Honshu (Usman et al., 2014; Buchs et al., 2015). Those comparisons indicate that the Outer Zone of SW Japan (Shimanto Belt) has been the main sediment source, with additional input from higher-grade metamorphic rocks of the Inner Zone. Turbidity currents during middle to late Pleistocene time evidently were routed into the Kumano Basin after fluvial transport through rivers on the Kii Peninsula and funneling through such transverse canyons as Anoriguchi Canyon (e.g., Blum and Okamura, 1992). Unlike sites farther seaward and downslope (e.g., C0001, C0018, C0006), no evidence exists for longitudinal transport into Kumano Basin from the collision zone between the Honshu and Izu-Bonin arcs system (e.g., Taira and Niitsuma, 1986; Fergusson, 2003) or via oblique transport from the Tenryu River through the Tenryu Canyon (Kawamura et al., 2009). Thus, routing of sandy turbidites into lower slope basins and the trench wedge has been decoupled during the Pleistocene from routing into the distal Kumano Basin (Usman et al., 2014; Buchs et al., 2015). Sediment provenance for the proximal turbidites of Astumi Knoll remains undocumented, but that supply was probably rerouted through Tenryu Canyon into the trench by uplift of the knoll.

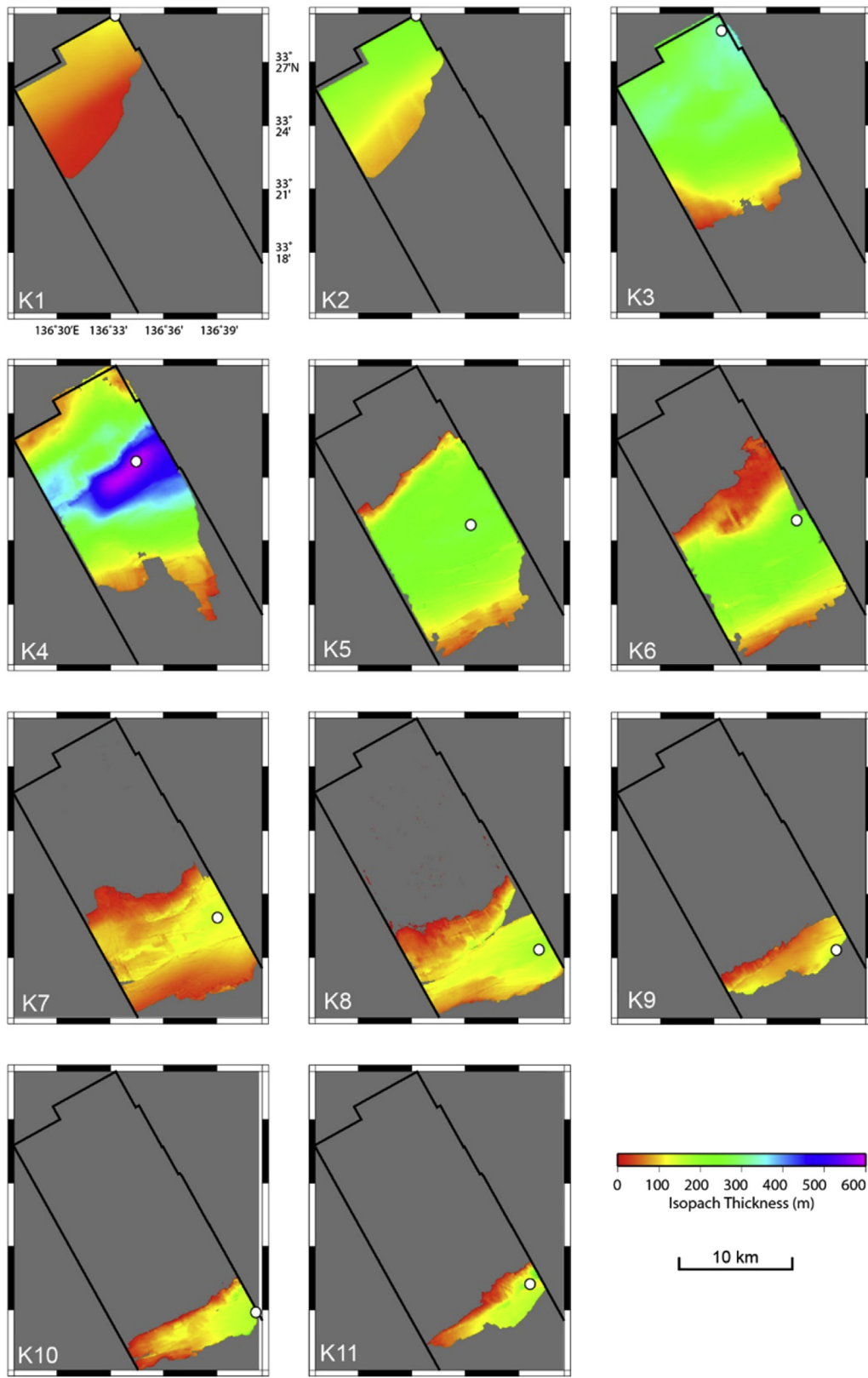


Fig. 12. Isopach maps of seismic sequences K1 through K11 showing the general widening and NW shift of the basin depocenter with time. White dots show thickest point of the basin during the isopach interval.

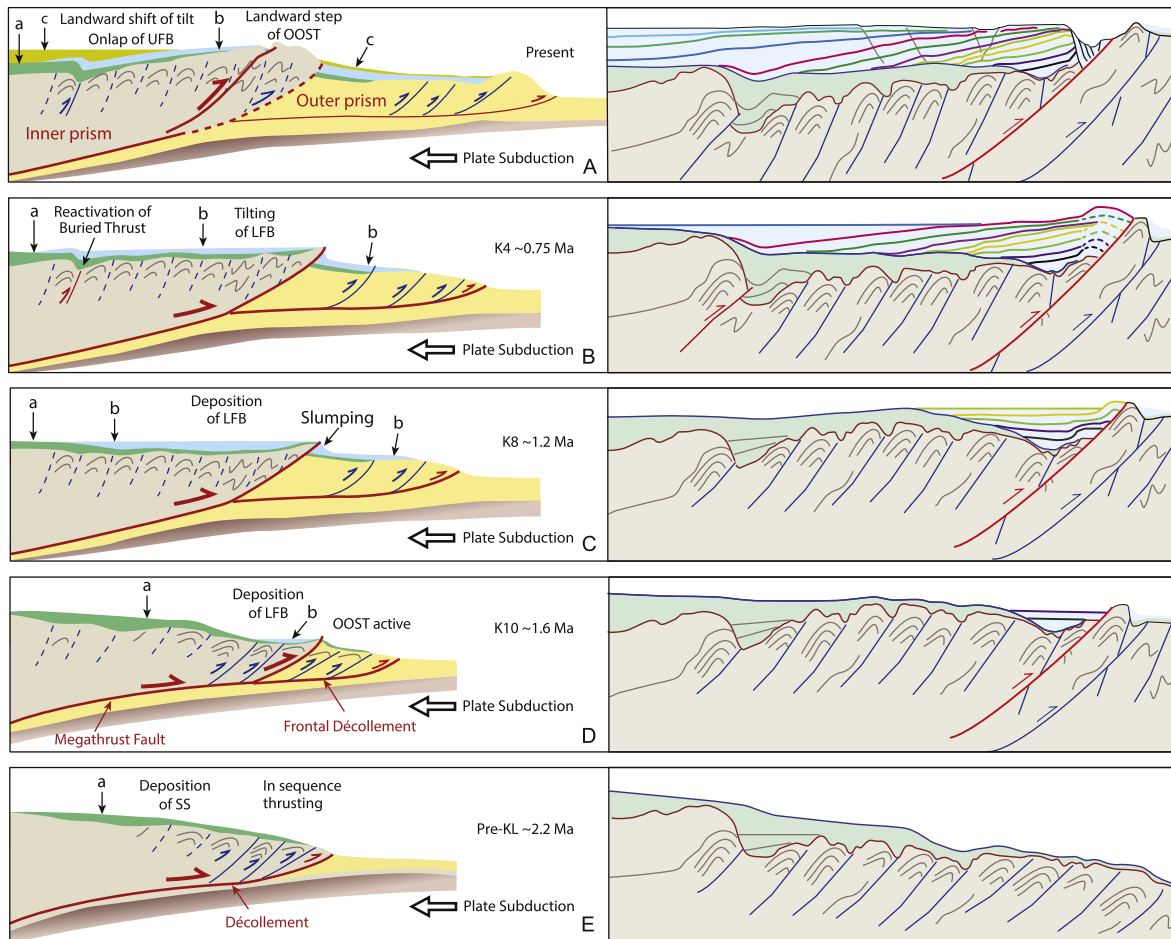


Fig. 13. Model of evolution of Kumano Basin. Left side: schematic model of entire frontal region; Right side: details of FAB evolution. A. Sedimentation of UFB; tilting of UFB and older units (present day). B. Continued tilting of basin sediments (K4 unit); reactivation of buried thrust in accretionary prism (~0.75 Ma). C. Deposition of LSB, sequence K8; tilting of LFB sediments (~1.2 Ma). D. Approximately 0.4 Ma after formation of OOST; sedimentation of LFB sequence K10 (~1.6 Ma). E. During deposition of slope sediments (~2.2 Ma). a = slope sediments; b = LFB sediments plus correlative slope sediments; c = UFB sediments plus correlative slope sediments. Color scheme is the same as Fig. 5 and 6. Modified from Moore et al. (2007).

6. Conclusions

The evolution of Kumano Basin in the forearc of Nankai Trough has been controlled by a combination of frontal subduction accretion, out-of-sequence thrust faulting, seamount collision, and glacio-eustatic forcing. Seismic reflection data reveal clear geometric patterns of infilling of the distal basin and landward migration of depocenters, whereas core data from two IODP sites demonstrate that nearly all of the basin-fill accumulated within the last 2.0 Ma. Formation of the distal basin along the Kumano transect was preceded by a long period of slow hemipelagic sedimentation on the lower trench slope (SS unit). That condensed section extended from ~3.79 Ma to ~1.67 Ma at Site C0002 and from ~5.6 Ma to ~0.9 Ma at Site C0009. Further to the NE at Atsumi Knoll, however, deformed channel-fill deposits as old as 2.4 Ma are preserved in the correlative slope-sediment acoustic unit. A critical phase in the basin's growth was triggered by uplift along the megasplay fault, which began around 2.0 Ma, allowing the forearc domain to evolve from a series of smaller, disjointed basins into its current broader physiography. A diachronous facies boundary separates the hemipelagic slope sediments of the SS unit from overlying silt and sand turbidites of the LSB unit, with sheet-like geometries characteristic of a basin-plain environment. The onlap pattern of reflection terminations migrated ~20 km toward the NW from Site C0002 (~1.67 Ma) to C0009 (~0.9 Ma) at a rate of

~30 km/Ma. Rapid influx of turbidite sand from detrital sources on the Kii Peninsula was probably enhanced by incision of a widespread system of transverse and oblique submarine canyons and slope gullies across the upper continental margin. Those conduits for gravity flows were probably enlarged by the effects of uplift and erosion of sediment sources on the nascent Japanese Islands, combined with Pleistocene intensification of glacio-eustatic forcing. Anomalous, late stage uplift of Astumi knoll near the basin's NE corner may have rerouted parts of the regional delivery system through Tenryu Canyon into the trench. When viewed in total, Kumano Basin provides an excellent case study of how forearc sedimentation can be intimately interwoven with accretionary-prism deformation, progressive landward tilting, and folding of the basin fill.

Acknowledgments

This project used data provided by the Integrated Ocean Drilling Program and International Ocean Discovery Program. We would like to thank the scientific parties of Expeditions 314, 315, 316, 319, 338 and 348 for sample collection and data acquisition. This work was supported by the U.S. National Science Foundation (grant # OCE-04551790), the U.S. Science Support Program (Post-expedition awards to G.F.M and M.B.U.), and the Swiss National Science Foundation (grant #133481 to M.S.).

We are grateful to Paradigm Geophysical and Landmark Graphics (Haliburton) for software grants that made this work possible. SOEST contribution # 9305.

Appendix A. Supplementary data

Supplementary data related to this article can be found at <http://dx.doi.org/10.1016/j.marpetgeo.2015.05.032>.

References

- Aoki, Y., Tamano, T., Kato, S., 1982. Detailed structure of the Nankai Trough from migrated seismic sections. In: Watkins, J.S., Drake, C.L. (Eds.), *Studies in Continental Margin Geology*, 34. AAPG Memoir, pp. 309–322.
- Ballesteros, M., Moore, G.F., Taylor, B., Rupert, S., 1988. Seismic-stratigraphic framework of the Lima and Yaquina forearc basins, Peru. *Proc. ODP Init. Repts* 112, 77–90.
- Bangs, N.L.B., Moore, G.F., Gulick, S.P.S., Pangborn, E.M., Tobin, H.J., Kuramoto, S., Taira, A., 2009. Broad, weak regions of the Nankai Megathrust and implications for shallow coseismic slip. *Earth Planet. Sci. Lett.* 284, 44–49.
- Bangs, N.L.B., Hornbach, M.J., Moore, G.F., Park, J.-O., 2010. Massive methane release triggered by seafloor erosion offshore southwestern Japan. *Geology* 38, 1019–1022.
- Beaudry, D., Moore, G.F., 1985. Seismic stratigraphy and Cenozoic evolution of west Sumatra fore-arc Basin. *AAPG Bull.* 69, 742–759.
- Berglar, K., Gaedicke, C., Lutz, R., Franke, D., Djajadihardja, Y.S., 2008. Neogene subsidence and stratigraphy of the Simeulue forearc basin, Northwest Sumatra. *Mar. Geol.* 253, 113.
- Blum, P., Okamura, Y., 1992. Pre-Holocene sediment dispersal systems and effects of structural controls and Holocene sea-level rise from acoustic facies analysis: SW Japan forearc. *Mar. Geol.* 108, 295–322.
- Boston, B., Barnes, J., Moore, G.F., 2011. Buried accretionary thrusts beneath the Kumano forearc basin, SW Japan. In: Abstract T51F-2413 Presented at 2011 Fall Meeting, AGU, San Francisco, CA, 5–9 Dec.
- Buchs, D.M., Cukur, D., Masago, H., Garbe-Schönberg, D., 2015. Sediment flow routing during formation of forearc basins: constraints from integrated analysis of detrital pyroxenes and stratigraphy in the Kumano Basin. *Jpn. Earth Planet. Sci. Lett.* 414, 164–175.
- Burgreen, B., Graham, S., 2014. Evolution of a deep-water lobe system in the Neogene trench-slope setting of the East Coast Basin, New Zealand: lobe stratigraphy and architecture in a weakly confined basin configuration. *Mar. Petrol. Geol.* 54, 1–22.
- Chapp, E., Taylor, B., Oakley, A., Moore, G.F., 2008. A seismic stratigraphic analysis of Mariana forearc basin evolution. *Geochem. Geophys. Geosys* 9, Q10X02. <http://dx.doi.org/10.1029/2008GC001998>.
- Coulbourn, W.T., Moberly, R., 1977. Structural evidence of the evolution of fore-arc basins off South America. *Can. J. Earth Sci.* 14, 102–116.
- Dickinson, W.R., 1995. Forearc basins. In: Busby, C.J., Ingersoll, R.V. (Eds.), *Tectonics of Sedimentary Basins*. Blackwell, Cambridge, MA, pp. 221–261.
- Egawa, K., Furukawa, T., Saeki, T., Suzuki, K., Narita, H., 2013. Three-dimensional paleomorphologic reconstruction and turbidite distribution prediction revealing a Pleistocene confined basin system in the northeast Nankai Trough area. *AAPG Bull.* 97, 781–798.
- Expedition 314 Scientists, 2009. Expedition 314 site C002. In: Kinoshita, M., Tobin, H., Ashi, J., Kimura, G., Lallemand, S., Screateon, E., Curewitz, D., Masago, H., Moe, K.T., Expedition Scientists, E. (Eds.), *Proc. IODP 314/315/316. Integrated Ocean Drilling Program Management Int.*, Washington, DC.
- Expedition 315 Scientists, 2009. Expedition 315 site C0002. In: Kinoshita, M., Tobin, H., Ashi, J., Kimura, G., Lallemand, S., Screateon, E., Curewitz, D., Masago, H., Moe, K.T., Expedition Scientists, E. (Eds.), *Proc. IODP 314/315/316. Integrated Ocean Drilling Program Management Int.*, Washington, DC.
- Expedition 319 Scientists, 2010. Site C0009. *Integrated Ocean Drilling Program Management Int.*, Tokyo.
- Expedition 348 Scientists, 2014. NanTroSEIZE Stage 3: NanTroSEIZE Plate Boundary Deep Riser 3. *IODP Prel. Rept.*, 348. <http://dx.doi.org/10.2204/iodp.pr.348.2014>.
- Fergusson, C., 2003. Provenance of Miocene-pleistocene Turbidite Sands and Sandstones, Nankai Trough, ODP Leg 190. *Proc. ODP, Sci. Results* 190/196.
- Fujii, T., Nakamizu, M., Tsuji, Y., Namikawa, T., Okui, T., Kawasaki, M., Ochiai, K., Nishimura, M., Takano, O., 2009. Methane-hydrate occurrence and saturation confirmed from core samples, Eastern Nankai Trough, Japan. In: Collett, T., Johnson, A., Knapp, C., Boswell, R. (Eds.), *Natural Gas Hydrates—Energy Resource Potential and Associated Geologic Hazards: AAPG Memoir*, 89, pp. 385–400.
- Geiser, J., Geiser, P., Kligfield, R., Ratliff, R., Rowan, M., 1988. New applications of computer-based cross section construction: strain analysis, local balancing and subsurface fault prediction. *Mt. Geol.* 25, 47–59.
- Groshong, R.H., Bond, C., Gibbs, A., Ratliff, R., Wiltschko, D.V., 2012. Preface: structural balancing at the start of the 21st century: 100 years since Chamberlain. *J. Struct. Geol.* 41, 1–5.
- Gulick, S.P.S., Bangs, N.L.B., Moore, G.F., Ashi, J., Martin, K.M., Sawyer, D.S., Tobin, H.J., Kuramoto, S., Taira, A., 2010. Rapid forearc basin uplift and megasplay fault development from 3D seismic images of Nankai Margin off Kii Peninsula, Japan. *Earth Planet. Sci. Lett.* 300, 55–62.
- Guo, J., Underwood, M.B., Likos, W.J., Saffer, D.M., 2013. Apparent overconsolidation of mudstones in the Kumano Basin of southwest Japan: Implications for fluid pressure and fluid flow within a forearc setting. *Geochem. Geophys. Geosyst.* 14, 1023–1038. <http://dx.doi.org/10.1029/2012GC004204>.
- Hayman, N.W., Byrne, T.B., McNeill, L.C., Kanagawa, K., Kanamatsu, T., Browne, C.M., Schleicher, A.M., Huftile, G.J., 2012. Structural evolution of an inner accretionary wedge and forearc basin initiation, Nankai margin, Japan. *Earth Planet. Sci. Lett.* 353–354, 163–172.
- Heki, K., 2007. Secular, transient and seasonal crustal movements in Japan from a dense GPS array: Implications for plate dynamics in convergent boundaries. In: Dixon, T., Moore, J.C. (Eds.), *The Seismogenic Zone of Subduction Thrust Faults*. Columbia University Press, New York, pp. 512–539.
- Ike, T., Moore, G.F., Kuramoto, S., Park, J.-O., Kaneda, Y., Taira, A., 2008a. Tectonics and sedimentation around Kashinosaki Knoll: a subducting basement high in the eastern Nankai Trough. *Isl. Arc* 17, 358–375.
- Ike, T., Moore, G.F., Kuramoto, S., Park, J.-O., Kaneda, Y., Taira, A., 2008b. Variations in sediment thickness and type along the northern Philippine Sea Plate at the Nankai Trough. *Isl. Arc* 17, 342–357.
- Ingersoll, R.V., Busby, C.J., 1995. Tectonics of sedimentary basins. In: Ingersoll, R.V., Busby, C.J. (Eds.), *Tectonics of Sedimentary Basins*. Blackwell, Cambridge, pp. 1–51.
- Kameo, K., Jiang, S., 2013. Data report: calcareous nannofossil biostratigraphy of Site C0009, Expedition 319. In: Saffer, D., McNeill, L., Byrne, T., Araki, E., Toczko, S., Eguchi, N., Takahashi, K. (Eds.), *And the Expedition 319 Scientists, Proc. IODP, 330. Integrated Ocean Drilling Program Management International, Inc.*, Tokyo. <http://dx.doi.org/10.2204/iodp.proc.319.202.2013>.
- Kawamura, K., Ogawa, Y., Anma, R., Yokoyama, S., Kawakami, S., Dilek, Y., Moore, G.F., Hirano, S., Yamaguchi, A., Sasaki, T., 2009. Structural architecture and active deformation of the Nankai Accretionary Prism, Japan: submersible survey results from the Tenryu Submarine Canyon. *GSA Bull.* 121, 1629–1646.
- Kazuoka, O., Sugnuma, Y., Okada, K., Kameo, K., Head, M.J., Yoshida, T., Sugaya, M., Kameyama, S., Ogitsu, I., Nirei, H., Aida, N., Kumai, H., 2015. Stratigraphy of the Kazusa Group, Boso Peninsula: an expanded and highly-resolved marine sedimentary record from the Lower and Middle Pleistocene of central Japan. *Quat. Int.* <http://dx.doi.org/10.1016/j.quaint.2015.02.065> (in press).
- Kimura, G., Hashimoto, Y., Kitamura, Y., Yamaguchi, A., Koge, H., 2014. Middle Miocene swift migration of the TTT triple junction and rapid crustal growth in southwest Japan: a review. *Tectonics* 33, 1219–1238.
- Kimura, G., Moore, G.F., Strasser, M., Screateon, E., Curewitz, D., Streiff, C., Tobin, H., 2011. Spatial and temporal evolution of the megasplay fault in the Nankai Trough. *Geochem. Geophys. Geosystems* 12.
- Kinoshita, M., Tobin, H., Ashi, J., Kimura, G., Lallemand, S., Screateon, E.J., Curewitz, D., Masago, H., Moe, K.T., Scientists, t.E., 2009. *Proc. IODP, 314/315/316. Integrated Ocean Drilling Program Management International, Inc.*, Washington, DC <http://dx.doi.org/10.2204/iodp.proc.314315316.2009>.
- Kobayashi, K., Kasuga, S., Okino, K., 1995. Shikoku Basin and its margins. In: Taylor, B. (Ed.), *Back-arc Basins*. Plenum, New York, pp. 381–405.
- Kodaira, S., Kaneda, Y., Takahashi, N., Nakanishi, A., Miura, S., 2000. Subducted seamount imaged in the rupture zone of the 1946 Nankaido earthquake. *Science* 289, 104–106.
- Kopp, H., 2011. The Java convergent margin: structure, seismogenesis and subduction processes. *Geol. Soc. London Spec. Publ.* 355, 111–137.
- Laursen, J., Normark, W.R., 2003. Impact of structural and autocyclic basin-floor topography on the depositional evolution of the deep-water Valpariso forearc basin, central Chile. *Basin Res.* 201–222.
- Laursen, J., Scholl, D.W., von Huene, R., 2002. Neotectonic deformation of the central Chile margin: Deepwater forearc basin formation in response to hot spot ridge and seamount subduction. *Tectonics* 21, 2–1–2–27.
- Lutz, R., Gaedicke, C., Berglar, K., Schlömer, S., Franke, D., Djajadihardja, Y.S., 2011. Petroleum systems of the Simeulue forearc basin off Sumatra, Indonesia. *AAPG Bull.* 95, 1589–1616. <http://dx.doi.org/10.1306/01191110090>.
- Martin, K.M., Gulick, S.P.S., Bangs, N.L.B., Moore, G.F., Ashi, J., Park, J.-O., Kuramoto, S., Taira, A., 2010. Possible strain partitioning structure between the Kumano fore-arc basin and the slope of the Nankai Trough accretionary prism. *Geochem. Geophys. Geosystems* 11, Q0AD02. <http://dx.doi.org/10.1029/2009GC002668>.
- Matson, R.G., Moore, G.F., 1992. Structural Influences on forearc basin subsidence in the central Sumatra forearc basin. In: Watkins, J.S., Zhiqiang, F., McMillen, K.J. (Eds.), *Geology and Geophysics of Continental Margins*. AAPG, Tulsa, pp. 157–181.
- McNeill, L.C., Goldfinger, C., Kulm, L.D., Yeats, R.S., 2000. Tectonics of the Neogene Cascadia forearc basin: investigations of a deformed late Miocene unconformity. *Geol. Soc. Amer. Bull.* 112, 1209–1224.
- Mitchell, C., Graham, S.A., Suck, D.H., 2010. Subduction complex uplift and exhumation and its influence on Maastrichtian forearc stratigraphy in the Great Valley Basin, northern San Joaquin Valley, California. *GSA Bull.* 122, 2063–2078.
- Miyakawa, A., Saito, S., Yamada, Y., Tomaru, H., Kinoshita, M., Tsuji, T., 2014. Gas hydrate saturation at Site C0002, IODP Expeditions 314 and 315, in the Kumano Basin, Nankai trough. *Isl. Arc* 23, 142–156.

- Miyazaki, S.I., Heki, K., 2001. Crustal velocity field of southwest Japan: subduction and arc-arc collision. *J. Geophys. Res.* 106, 4305–4326.
- Moore, G.F., Kanagawa, K., Strasser, M., Dugan, B., Maeda, L., Toczko, S., IODP Exp. 338 Sci. Party, 2014. IODP Expedition 338: NanTroSEIZE Stage 3: NanTroSEIZE plate boundary deep riser 2. *Sci. Drill.* 17, 1–2.
- Moore, G.F., Strasser, M., 2015. Large Mass Transport Deposits in Kumano Basin, Nankai Trough, Japan. *Advances in Natural and Technological Hazard Research* (in press).
- Moore, G.F., Bangs, N.L., Taira, A., Kuramoto, S., Pangborn, E., Tobin, H.J., 2007. Three-dimensional splay fault geometry and implications for tsunami generation. *Science* 318, 1128–1131.
- Moore, G.F., Boston, B.B., Sacks, A.F., Saffer, D.M., 2013. Analysis of normal fault populations in the Kumano Forearc Basin, Nankai Trough, Japan: 1. Multiple orientations and generations of faults from 3-D coherency mapping. *Geochem. Geophys. Geosystems* 14, 1989–2002.
- Moore, G.F., Park, J.O., Bangs, N.L., Gulick, S.P., Tobin, H.J., Nakamura, Y., Saito, S., Tsuji, T., Yoro, T., Tanaka, H., Uraki, S., Kido, Y., Sanada, Y., Kuramoto, S., Taira, A., 2009. Structural and Seismic Stratigraphic Framework of the NanTroSEIZE Stage 1 Transect. *Proc. IODP 314/315/316*, pp. 1–46.
- Moore, G.F., Shipley, T.H., Stoffa, P.L., Karig, D.E., Taira, A., Kuramoto, S., Tokuyama, H., Suyehiro, K., 1990. Structure of the Nankai trough accretionary zone from Multichannel seismic-reflection data. *J. Geophys. Res.* 95, 8753–8765.
- Nakanishi, A., Kodaira, S., Miura, S., Ito, A., Satao, T., Park, J.-O., Kido, Y., Kaneda, Y., 2008. Detailed structural image around splay-fault branching in the Nankai subduction seismogenic zone: results from a high-density ocean bottom seismic survey. *J. Geophys. Res.* 113, B03105. <http://dx.doi.org/10.1029/2007jb004974>.
- Noguchi, S., Shimoda, N., Takano, O., Oikawa, N., Inamori, T., Saeki, T., Fujii, T., 2011. 3-D internal architecture of methane hydrate-bearing turbidite channels in the eastern Nankai Trough. *Jpn. Mar. Petrol. Geol.* 28, 1817–1828.
- Okino, K., Shimakawa, Y., Nagakoa, S., 1994. Evolution of the Shikoku Basin. *J. Geomagn. Geoelectr.* 46, 463–479.
- Omura, A., Ikehara, K., 2010. Deep-sea sedimentation controlled by sea-level rise during the last deglaciation, an example from the Kumano Trough, Japan. *Mar. Geol.* 274, 177–186.
- Omura, A., Ikehara, K., Sugai, T., Shirai, M., Ashi, J., 2012. Determination of the origin and processes of deposition of deep-sea sediments from the composition of contained organic matter: an example from two forearc basins on the landward flank of the Nankai Trough. *Jpn. Sed. Geol.* 249–250, 10–25.
- Pape, T., Geprágs, P., Hammerschmidt, S., Wintersteller, P., Wei, J., Fleischmann, T., Bohrmann, G., Kopf, A.J., 2014. Hydrocarbon seepage and its sources at mud volcanoes of the Kumano forearc basin, Nankai Trough subduction zone. *Geochem. Geophys. Geosystems* 15, 2180–2194.
- Paquet, F., Proust, J.N., Barnes, P.M., Pettinga, J.R., 2011. Controls on active forearc basin stratigraphy and sediment fluxes: the Pleistocene of Hawke Bay, New Zealand. *Geol. Soc. Am. Bull.* 123, 1074–1096.
- Park, J.O., Kaneda, Y., Tsuru, T., Kodaira, S., Cummins, P.R., 2002. Splay fault branching along the Nankai subduction zone. *Science* 297, 1157–1160.
- Park, J.O., Kodaira, S., Takahashi, N., Kinoshita, H., Tsuru, T., Kaneda, Y., Kono, Y., 1999. A subducting seamount beneath the Nankai accretionary prism off Shikoku, southwestern Japan. *Geophys. Res. Lett.* 26, 931–934.
- Pickering, K.T., Souter, C., Oba, T., Taira, A., Schaaf, M., Platzman, E., 1999. Glacio-eustatic control on deep-marine clastic forearc sedimentation, Pliocene-mid-Pleistocene (ca 1180–600 ka) Kazusa Group, SE Japan. *J. Geol. Soc. Lond.* 156, 125–136.
- Pickering, K.T., Underwood, M.B., Saito, S., Naruse, H., Kutterolf, S., Scudder, R., Park, J.-O., Moore, G.F., Slagle, A., 2013. Depositional architecture, provenance, and tectonic/eustatic modulation of Miocene submarine fans in the Shikoku Basin: results from Nankai Trough Seismogenic Zone Experiment. *Geochem. Geophys. Geosyst* 14, 1722–1739.
- Raimbourg, H., Augier, R., Famin, V., Gadenne, L., Palazzin, G., Yamaguchi, A., Kimura, G., 2014. Long-term evolution of an accretionary prism: the case study of the Shimanto Belt, Kyushu, Japan. *Tectonics* 33, 936–959.
- Ramirez, S., Gulick, S.P.S., Hayman, N.W., 2015. Early sedimentation and deformation in the Kumano forearc basin linked with Nankai accretionary prism evolution, southwest Japan. *Geochem. Geophys. Geosyst.* <http://dx.doi.org/10.1002/2014GC005643>.
- Rowan, M.G., Ratliff, R.A., 2012. Cross-section restoration of salt-related deformation: best practices and potential pitfalls. *J. Struct. Geol.* 41, 24–37.
- Sacks, A., Saffer, D.M., Fisher, D., 2013. Analysis of normal fault populations in the Kumano basin, Nankai Trough, Japan: 2. Principal axes of stress and strain from inversion of fault orientations. *Geochem. Geophys. Geosystems* 14, 1973–1988.
- Screaton, E., Kimura, G., Curewitz, D., Moore, G., Expedition 316 Scientists, 2009. Interactions between deformation and fluids in the frontal thrust region of the NanTroSEIZE transect offshore the Kii Peninsula, Japan: results from IODP Expedition 316 Sites C0006 and C0007. *Geochem. Geophys. Geosystems* 10, Q0AD01.
- Saffer, D., McNeill, L.C., Byrne, T., Araki, E., Toczko, S., Eguchi, N., Takahashi, K., Expedition Scientists, E., 2010. NanTroSEIZE Stage 2: NanTroSEIZE riser/riserless observatory. In: *Proc. IODP. Integrated Ocean Drilling Program Management International, Inc.*, Tokyo.
- Sdrolias, M., Roest, W.R., Müller, R.D., 2004. An expression of Philippine sea plate rotation: the Parece Vela and Shikoku basins. *Tectonophysics* 394, 69–86.
- Seno, T., Stein, S., Gripp, A.E., 1993. A model for the motion of the Philippine Sea plate consistent with NUVEL-1 and geological data. *J. Geophysical Res.* 98, 17,941–17,948.
- Shirai, M., Hayashizaki, R., 2013. Transport process of sand grains from fluvial to deep marine regions estimated by luminescence of feldspar: example from the Kumano area, central Japan. *Isl. Arc* 22, 242–257.
- Shirai, M., Omura, A., Wakabayashi, T., Uchida, J.-I., Ogami, T., 2010. Depositional age and triggering event of turbidites in the western Kumano Trough, central Japan during the last ca. 100 years. *Mar. Geol.* 271, 225–235.
- Speed, R.C., Torrini, R.J., Smith, P.L., 1989. Tectonic evolution of the Tobago Trough forearc basin. *J. Geophys. Res.* 94, 2913–2936.
- Strasser, M., Moore, G.F., Kimura, G., Kitamura, Y., Kopf, A.J., Lallemand, S., Park, J.-O., Screaton, E.J., Su, X., Underwood, M.B., Zhao, X., 2009. Origin and evolution of a splay fault in the Nankai accretionary wedge. *Nat. Geosci.* 2, 648–652.
- Strasser, M., Moore, G.F., Kimura, G., Kopf, A.J., Underwood, M.B., Guo, J., Screaton, E.J., 2011. Slumping and mass transport deposition in the Nankai fore arc: evidence from IODP drilling and 3-D reflection seismic data. *Geochem. Geophys. Geosyst* 12, Q0AD13. <http://dx.doi.org/10.1029/2010GC003431>.
- Strasser, M., Dugan, B., Kanagawa, K., Moore, G.F., Expedition 338 Scientists, 2014. Site C0002. In: *Proc. IODP, 338. IODP, Yokohama.* <http://dx.doi.org/10.2204/iodp.proc.338.103.2014>.
- Struss, I., Artilles, V., Cramer, B., Winsemann, J., 2008. The petroleum system in the Sandino forearc basin, offshore Western Nicaragua. *J. Petrol. Geol.* 31, 221–244.
- Susilohadi, S., Gaedicke, C., Ehrhardt, A., 2005. Neogene structures and sedimentation history along the Sunda forearc basins off Sumatra and southwest Java. *Mar. Geol.* 219, 133–154. <http://dx.doi.org/10.1016/j.margeo.2005.05.001>.
- Taira, A., 2001. Tectonic evolution of the Japanese Island arc system. *Ann. Rev. Earth Planet. Sci.* 29, 109–134.
- Taira, A., Katto, J., Tashiro, M., Okamura, M., Kodama, K., 1988. The Shimanto Belt in Shikoku Japan: evolution of a Cretaceous to Miocene accretionary prism. *Mod. Geol.* 12, 5–46.
- Taira, A., Niitsuma, N., 1986. Turbidite sedimentation in the Nankai Trough as interpreted from magnetic fabric, grain size, and detrital modal analyses. In: Kagami, H., Karig, D.E., Coulbourn, W.T., et al. (Eds.), *Init. Repts. DSDP. U.S. Govt. Printing Office, Washington*, pp. 611–632.
- Takano, O., Itoh, Y., Kusumoto, S., 2013. Variation in forearc basin configuration and basin-filling depositional systems as a function of trench slope break development and strike-slip movement: Examples from the Cenozoic Ishikari-Sanriku-Oki and Tkai-Oki-Kumano-Nada forearc basins, Japan. In: Itoh, Y. (Ed.), *Mechanism of Sedimentary Basin Formation – Multidisciplinary Approach on Active Plate Margins*. InTech, Rijeka. <http://dx.doi.org/10.5772/56751>.
- Torrini, R.J., Speed, R.C., 1989. Tectonic wedging in the fore-arc basin - accretionary prism transition, Lesser Antilles fore-arc. *J. Geophys. Res.* 94, 10549–10584.
- Tsuji, Y., Namikawa, T., Fujii, T., Hayashi, M., Kitamura, R., Nakamizu, M., Ohbi, K., Saeki, T., Yamamoto, K., Inamori, T., Oikawa, N., Shimizu, S., Kawasaki, M., Nagakubo, S., Matsushima, J., Ochiai, K., Okui, T., 2009. Methane-hydrate occurrence and distribution in the eastern Nankai Trough, Japan: findings of the Tokai-oki to Kumano-nada methane-hydrate drilling program. *AAPG Mem.* 89, 228–246.
- Underwood, M.B., Moore, G.F., 2012. Evolution of sedimentary environments in the subduction zone of southwest Japan: recent results from the NanTroSEIZE Kumano transect. In: Busby, C.J., Azor, A.P. (Eds.), *Tectonics of Sedimentary Basins: Recent Advances*. Wiley-Blackwell, New York, pp. 310–326.
- Underwood, M.B., Moore, G.F., Taira, A., Klaus, A., Wilson, M.E.J., Fergusson, C.L., Hirano, S., Steurer, J., 2003. Sedimentary and tectonic evolution of a trench-slope basin in the Nankai subduction zone of southwest Japan. *J. Sed. Res.* 73, 589–602.
- Usman, M.O., Masago, H., Winkler, W., Strasser, M., 2014. Mid-Quaternary decoupling of sediment routing in the Nankai forearc revealed by provenance analysis of turbiditic sands. *Int. J. Earth Sci.* 103, 1141–1161.
- von Huene, R., 2008. When seamount subduct. *Science* 321, 1165–1166.
- Wang, K., Hu, Y., 2006. Accretionary prisms in subduction earthquake cycles: the theory of dynamic Coulomb wedge. *J. Geophys. Res.* 111, B06410. <http://dx.doi.org/10.1029/2005JB004094>.
- Williams, T.A., Graham, S.A., 2013. Controls on forearc basin architecture from seismic and sequence stratigraphy of the Upper Cretaceous Great Valley Group, central Sacramento Basin, California. *Int. Geol. Rev.* 55, 2030–2059.